Appl. Phys. B 57, 145–158 (1993)

Applied Physics B Photophysics and Laser Chemistry

Pulsed-Laser Sputtering of Atoms and Molecules. Part I: Basic Solutions for Gas-Dynamic Effects*

R. Kelly, A. Miotello

Dipartimento di Fisica dell'Università di Trento and Consorzio Interuniversitario Nazionale Fisica della Materia, I-38050 Povo, Trento, Italy (Fax: +39-461/881696)

Received 15 October 1992/Accepted 8 April 1993

Abstract. When gases are released from a pulsed nozzle or when solids are sputtered with intense laser pulses, effusion-like expansions take place which terminate abruptly. The resulting gas-dynamic processes depend on γ, the heat capacity ratio, as well as on whether particles backscattered to the effusing surface are subject to recondensation or reflection. Certain aspects of these terminating expansions have already been treated but we consider it appropriate to examine the problem further. In particular the following topics are emphasized. (a) Following previous work, the expansions are shown to consist of a series of regions separated by lines of contact, i.e. abrupt changes of slope. (b) For conditions of recondensation, there are two regions separated by one line of contact, the first region lying in part behind the effusing surface. For conditions of reflection, there are three regions, the first of which begins at the surface. Both types of expansion terminate with a region which is a remanent of the release process. (c) The near-surface region under conditions of reflection permits an analytical approximation valid for all γ in which the sound speed is invariant with distance and the flow velocity is linear with distance. (d) The surface itself under conditions of recondensation permits an analytical approximation valid for all γ for the sound speed. More generally the near-surface region can be resolved by the method of Stanyukovich. (e) The various analytical solutions and approximations are shown to compare favorably with numerical results. (f) Plots of density and flow velocity versus distance are found to be roughly independent of γ, thence of the nature of the sputtered particles. (g) Tabulated results are presented to enable a more general use of gas-dynamic ideas.

PACS: 79.20, 81.60, 47.10

One-dimensional expansions which do not terminate, also termed *centered waves* [2], have been well understood since the appearance of the book (actually a doctoral thesis) of Stanyukovich in 1959 [3] but have taken on a new significance in view of current work on emission of gas from nozzles and on laser sputtering of solids [4]. We have subsequently noted [5] that the solutions have two basic forms, depending on whether the expansions originate from the removal of the wall of a semi-infinite reservoir or from an effusion-like process. From an experimental point of view, wall removal occurs when, for example, particles incident on a solid cause instantaneous bond breaking at the surface, while effusion-like behaviour occurs when, for example, a laser beam heats the surface to a sufficiently high temperature.

Let us recall the mathematical expressions which describe non-terminating expansions into vacuum [5]. This is the "simple expansion regime" of [2] or the "flow phase" of [6]:

wall removal

$$a = \frac{2}{\gamma+1} a_0 \left(1 - \frac{\gamma-1}{2} \frac{x}{a_0 t}\right), \tag{1a}$$

$$u = \frac{2}{\gamma+1} a_0 \left(1 + \frac{x}{a_0 t}\right), \qquad \hat{u} = \frac{2a_0}{\gamma-1}, \tag{1b}$$

effusion-like process

$$a = u_K \left(1 - \frac{\gamma-1}{\gamma+1} \frac{x}{u_K t}\right), \tag{1c}$$

$$u = u_K \left(1 + \frac{2}{\gamma+1} \frac{x}{u_K t}\right), \qquad \hat{u} = \frac{\gamma+1}{\gamma-1} u_K . \tag{1d}$$

Here a is the sound speed, u is the flow velocity, x is distance normal to the wall or effusing surface, t is time, and $\gamma = C_p/C_V$ is the heat capacity ratio (also termed *adiabatic coefficient* [2]). $\hat{u}$ is the maximum possible value of u, as occurs at the *expansion front* where we have $a = 0$. a_0 characterizes the undisturbed reservoir, $2a_0/(\gamma+1)$ characterizes the surface of the reservoir, and $u_K = a_K$ characterizes the outer boundary of the *Knudsen layer* (KL) formed by the effusing particles [3]. The corresponding density is given by

$$\varrho \propto a^{2/(\gamma-1)} \tag{1e}$$

* For Part II, which deals with recondensation, see [1]

Table 1. Various numerical constants relevant to terminating expansions

Species	Heat capacity ratio, γ	The exponent in the relation $P = A^{2/(\gamma-1)}$ (3c)	The value of $\check{U}$ with recondensation, $\check{U} = -(3-\gamma)/(\gamma-1)$ (5b)	The value of A_0 with recondensation, $A_0 = (3-\gamma)/(\gamma+1)$ (6b)	The value of A_0^{ref} with reflection, $A_0^{\text{ref}} = (3-\gamma)/2$ (11b)
Atoms	5/3	3	−2	1/2	2/3
Rotating diatomics	7/5	5	−4	2/3	4/5 [a]
Diatomics which both rotate and vibrate	9/7 [c]	7	−6	3/4	6/7 [b]
Intermediate molecules	11/9 [c]	9	−8	4/5	8/9
Large molecules which both rotate and vibrate	1	∞	$-\infty$	1	1

[a] Agrees with (A10) of [2]
[b] Agrees with (A11) of [2]
[c] Useful also for hot molecules (Table 2 of [9])

for any adiabatic, reversible, isentropic process involving a perfect gas. Values of $2/(\gamma-1)$ are included in Table 1.

We would recall that the KL is the near-surface region where the emitted particles come to equilibrium with each other [7–10]. The equilibration process has a number of consequences, including the development of a formal flow velocity, a slight cooling, and a scattering of some particles towards the emitting surface. In the most rigorous sense, a KL is infinitely thick [7] but in practice it can be taken as having the thickness appropriate to 3 to 5 mean free paths [11,12]. This in turn means that, when a KL is coupled to an expansion extending over many mean free paths, the KL can be taken as having zero thickness and therefore becomes a boundary condition. This will be true of the present work.

For $\gamma = 1$, Sibold and Urbassek [2] have shown that (1d) remains valid but that (1c) and (1e) are replaced with

$$a = u_K , \quad \varrho = \varrho_K \exp(-x/u_K t) , \tag{2a}$$

$$a \propto \varrho^{(\gamma-1)/2} = 1 . \tag{2b}$$

Equation (2a) follows easily by taking the limit of

$$\left(1 - \frac{\gamma-1}{\gamma+1}\frac{x}{u_K t}\right)^{2/(\gamma-1)}$$

for $\gamma \to 1$. ϱ_K characterizes the outer boundary of the KL. These unusual relations are discussed further in Sect. 1.1.

One-dimensional expansions which terminate are probably more important from an experimental point of view, because most work with nozzles and lasers is done under conditions of pulsed release. The same work by Stanyukovich [3] showed how to resolve them for *wall removal* and it was subsequently proposed that the sputtering of condensed gases such as Ar(s) or Kr(s) by heavy ions proceeds as if a wall were removed [13,14]. *Effusion-like processes* occur when gases are released from a pulsed nozzle as well as when solids are sputtered with intense laser pulses. We here recall that explicit photographs of laser-sputtered particles have recently become available [4,15] and the expansions were found to be reasonably one-dimensional and with a more or less well-defined *contact front* (Figs. 1a, 1b). (A *contact front* is the analog of an *expansion front* when there is an ambient gas. Provided the driving gas density, here ϱ_K, is sufficiently large, however, it is not necessary to make a distinction.) We also note that there are two limiting variants both for wall removal and for effusion-like processes. When the expansion is due to wall removal one must decide whether particles scattered towards the back of the reservoir recondense or reflect. Likewise, when the expansion is effusion-like one must decide whether, at the moment when the release process terminates, particles scattered towards the effusing surface recondense (Fig. 2a) or reflect (Fig. 2b). This leads to a total of four basic types of terminating expansion, as outlined in Table 2.

Solutions thus far available for terminating expansions include that for *wall removal* with $\gamma = 5/3$ and reflection [14]. For *effusion-like processes*, explicit solutions are available with $\gamma = 5/3$, $7/5$, and $9/7$, and either recondensation or reflection [2,6,16]. Tabulated values of a and u are available only for $\gamma = 5/3$ and reflection [16], while comparisons of analytical with numerical results have yet to be made. Only the solutions for $\gamma = 5/3$ and reflection were made by the method of Stanyukovich [3], which is perhaps the simplest approach currently known.

We wish here to extend the available information for one-dimensional effusion-like expansions which terminate beyond what is available in previous work [2,6,16] and using, in so doing, what we hope are the simplest possible mathematical methods. Specifically, we consider processes with γ taking on the values 5/3, 7/5, 9/7, 11/9, and 1 (Table 1), with the argument developed essentially as follows. (a) Following Sibold and Urbassek [2], we emphasize that terminating expansions consist of a series of regions separated by *lines of contact* (LOC), i.e. abrupt changes of slope in ϱ and u. A LOC is also known as a *weak discontinuity* or a *weak singularity* [2]. (b) For conditions of recondensation, there are two regions separated by one LOC, the first region lying in part behind the effusing surface. For conditions of reflection, there are three regions separated by two LOC, the first region beginning at the surface. Both types of expansion terminate with a region which is a remanent of the release process and progresses to the *expansion front*. (c) The near-surface region (i.e. region I) under conditions of reflection permits an analytical approximation valid for all γ in which a is invariant with distance and u is linear with distance. (d) The surface itself under conditions of recondensation permits an analytical approximation valid for all γ for a,

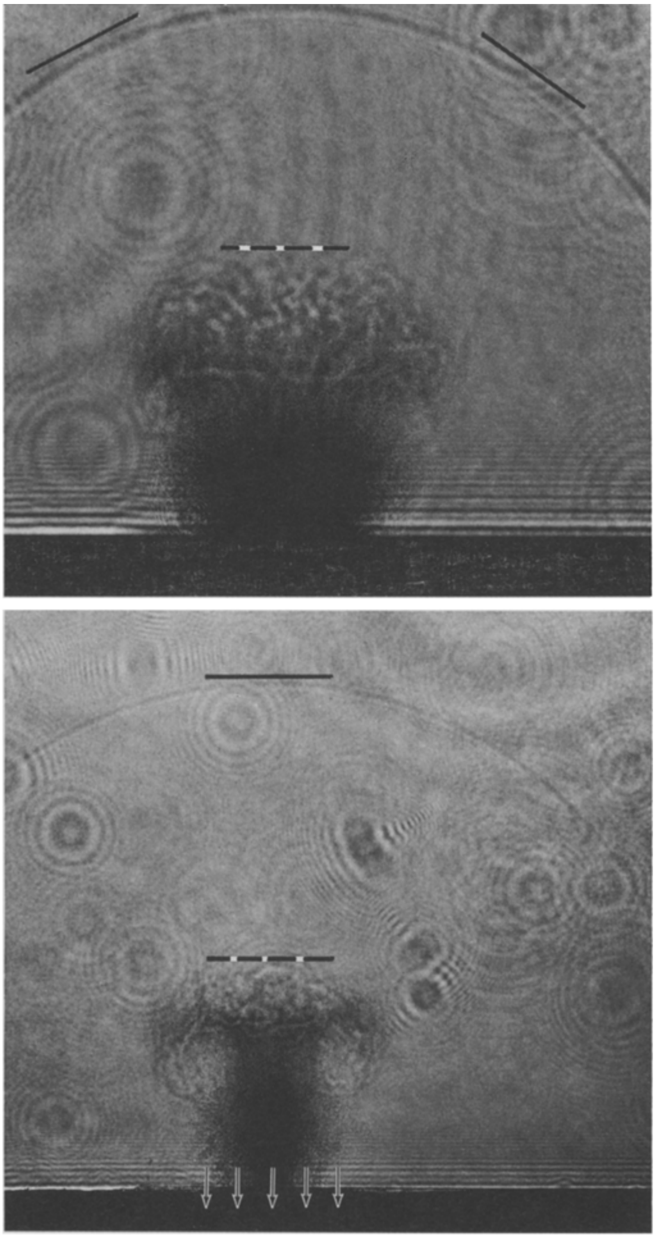

Fig. 1a, b. Polymethylmethacrylate targets with a thickness of 700 µm were exposed to 5 laser pulses (248 nm, ~20 ns, diameter 700 µm, 2.1 J/cm^2, normal incidence) in air [4, 15]. The emitted heavy particles, and the shock wave caused by the emitted light particles, were photographed by firing parallel to the target surface a second ("probe") laser (596 nm, ~1 ns). The contact front of the heavy particles (similar to an expansion front) is marked with a *dashed line*, the shock wave with a *solid line*. The contact front of the light particles is not imaged. **a** Delay of 2.9 µs; **b** delay of 4.9 µs and reduction of magnification by factor of 0.61. The *arrows* represent the recondensation process

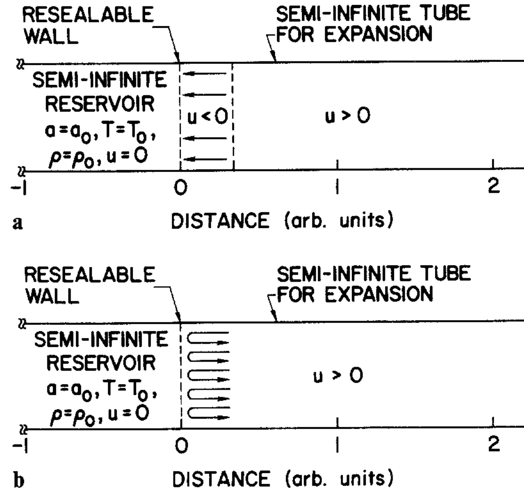

Fig. 2. a A terminating, effusion-like expansion with *recondensation*. Gas in a semi-infinite reservoir effuses into a vacuum from $t = 0$ (when the wall effectively becomes porous and u is everywhere positive) to $t = \tau_r$ (when the wall is resealed and u becomes negative near the surface). The resealing is equivalent to the termination of the release process; **b** Same but for a terminating, effusion-like expansion with *reflection*

but not for u. More generally, the near-surface region (i.e. region II) can be resolved by the method of Stanyukovich [3], which has the advantage of simplicity compared with the method of characteristics as used in [2]. (e) The various analytical solutions and approximations are compared with numerical results. No errors are found, although (A12), (A13), (A16), and (A17) of [2] are found to lack an important simplification. (f) Plots of ϱ versus x and u versus x are found to be roughly independent of γ, thence of the nature of the sputtered particles. This situation was not previously recognized and should facilitate the analysis of information as in Fig. 1. (g) Finally, we give extensive tabulated results, including for the previously untreated case of $\gamma = 11/9$ and partly treated case of $\gamma = 1$, to enable a more general use of gas-dynamic ideas.

Our justification for extending the understanding of terminating expansions to values of γ other than 5/3 is that in real examples of pulsed-laser sputtering there are well-defined roles for diatomics, as with bombardments of the superconductor $YBa_2Cu_3O_{7-x}$ [17], and for large molecules, such as the monomers and monomer fragments released in the bombardment of polymers [18, 19]. Some of the differences are minor: for example, it will be seen in Figs. 4 and 5 to matter little to the profiles of ϱ versus x or u versus x whether γ is 7/5, 11/9 or 1. On the other hand, some of the differences are quite important: for example, the quan-

Table 2. Classification of terminating expansions

Basic process	Knudsen layer?	Behaviour at surface or back of reservoir	Condensation efficiency	Suggested name[a]
Wall removal	No	Recondensation	1	Outflow with recondensation
	No	Reflection	0	Outflow with reflection
Effusion-like	Yes	Recondensation	1	Effusion with recondensation
	Yes	Reflection	0	Effusion with reflection

[a] There is apparently no established terminology to describe the various types of expansion, with a different choice being made, for example, in [4, 6, 16]

tity of recondensation, which plays a fundamental role when pulsed-laser sputtering is used to fashion integrated circuits, increases by a factor of 3 as γ passes from 5/3 to 1 [1, 20].

We do not intend to discuss the problems that occur at low densities and the particles go into *free flight* [5, 21]. In effect, the flow equations and any solutions derived from them, break down. This breakdown is less serious with a and ϱ since these in any case evolve to zero as the distance increases but rather more serious with the temperature T. Indeed, T finally begins to *increase* (instead of decrease!) with distance at low enough densities [22, 23] and temperatures parallel and perpendicular to the direction of flow cease to be equal [22]. Nor do we discuss the following: (a) three-dimensionality, as must inevitably occur far enough away from the target [20, 24, 25]; (b) the presence, for whatever reason, of ions amongst the sputtered particles [26, 27]; (c) the presence of a recondensation Knudsen layer, whenever backscattered particles are absorbed by the surface, in which the particles cease to be in equilibrium [28, 29].

1 Solution of the Problem of a Terminating, Effusion-Like Expansion

1.1 Underlying Relations

For $\gamma \neq 1$ we use the flow equations in their usual form. We will express the variables adimensionally and therefore write

$$A = a/u_K, \quad U = u/u_K, \quad P = \varrho/\varrho_K,$$
$$X = x/u_K\tau_r, \quad \Upsilon = t/\tau_r,$$

τ_r being the length of the release ("r") process. τ_r could also be said to define the instant when the porous wall is resealed (Fig. 2) or when the expansion terminates, and is not necessarily the same as the laser pulse length τ. u_K and ϱ_K, which characterize the KL boundary, can be understood in terms of KL theory, as pioneered by Ytrehus [7] and Cercignani [8] and as first applied to pulsed-laser sputtering by one of the present authors [9, 10]. The flow equations [2, 16] thus become:

$$\frac{\partial A}{\partial \Upsilon} + U\frac{\partial A}{\partial X} + \frac{(\gamma-1)A}{2}\frac{\partial U}{\partial X} = 0, \quad \text{(continuity equation)} \tag{3a}$$

$$\frac{\partial U}{\partial \Upsilon} + U\frac{\partial U}{\partial X} + \frac{2A}{\gamma-1}\frac{\partial A}{\partial X} = 0, \quad \text{(Euler equation)} \tag{3b}$$

and that for density (1e) becomes

$$P = A^{2/(\gamma-1)}, \tag{3c}$$

with an equalitiy instead of proportionality.

For $\gamma = 1$ Sibold and Urabassek [2] have argued that there is a physical problem in that the gas particles leave the surface with a uniform T no matter what is the value of γ. But if there is a large number of degrees of freedom, as when $\gamma \longrightarrow 1$, the energy tends to infinity. This requires the relation $P = A^{2/(\gamma-1)}$ to be replaced with [cf. (2b)]

$$A = P^{(\gamma-1)/2} = 1, \tag{4a}$$

the system becomes isothermal, and A ceases to be variable. Equations (3a) and (3b) must therefore be written in terms of density [2]:

$$\partial P/\partial\Upsilon + (\partial/\partial X)(PU) = 0, \quad \text{(continuity equation)} \tag{4b}$$

$$\partial U/\partial\Upsilon + U\partial U/\partial X + P^{-1}\partial P/\partial X = 0, \quad \text{(Euler equation; } \gamma = 1) \tag{4c}$$

The Euler equation in this form is valid only for $\gamma = 1$ and only with adimensional variables. We here recall that a better known form, e.g. (4) of [2] and (3b) of [6], is the following:

$$\partial U/\partial\Upsilon + U\partial U/\partial X + (A^2/P)\partial P/\partial X = 0. \quad \text{(Euler equation; all } \gamma) \tag{4d}$$

To help in comparing the present work with [2], we note the following major notational differences:

here	a	$\check{X}$	X_{I}	X_{II}	$\hat{X}$
[2]	c	$x_{\min}$	C_2^+	C_1^+	$x_{\max}$

here	$\frac{2\check{A}}{\gamma-1} + \check{U}$	$\frac{2A_{\mathrm{I}}}{\gamma-1} + U_{\mathrm{I}}$	$\frac{2A_{\mathrm{II}}}{\gamma-1} + U_{\mathrm{II}}$
[2]	$-2\Gamma_1^-$	$2\Gamma_2^+$	$2\Gamma_1^+$

1.2 Results for a Terminating, Effusion-Like Expansion with Recondensation

At the moment that an effusion-like expansion terminates there is an abrupt change of boundary conditions at the effusing surface. When particles backscattered to the surface undergo *recondensation*, U falls from 1 to a negative value $-U_0$ and A falls from 1 to A_0. As already noted [2, 6] the expansion, as a result of these changes, evolves from that described by (1c) and (1d) to one with two parts (Fig. 3). These will be termed *region II* (the "post-pulse regime" of [2]) and *region III* (the "simple expansion regime" of [2] or "flow phase" of [6]), such that region II begins at the *virtual expansion front* or minimum X at $\check{X}$, continues through the surface at $X = 0$, and ends with an abrupt

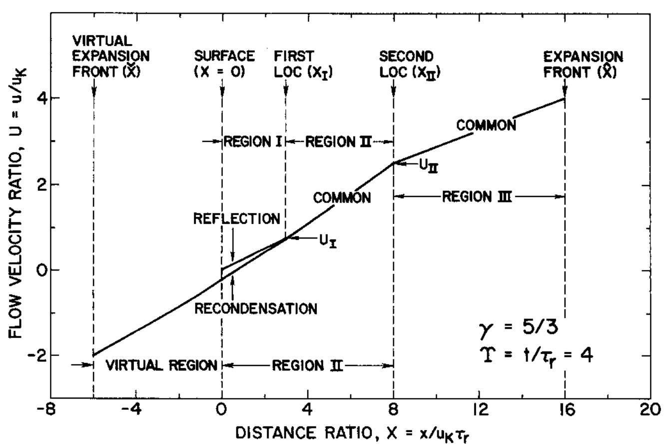

Fig. 3. Flow velocity *vs* distance for $\gamma = 5/3$ and $\Upsilon = 4$. Shown are the expansion fronts, lines of contact (LOC), and regions. For *recondensation* region II could also be regarded as extending from the virtual expansion front ($\check{X}$) to the second LOC (X_{II})

change of slope at the second LOC at X_{II}. Region III begins at X_{II} and ends at the *real expansion front* or maximum X at $\hat{X}$. The existence of two instead of three parts, as when there is reflection (Fig. 3), can be explained as follows. The first LOC for reflection arises from the lower part of the disturbance at the surface and has a positive velocity given by $dX_{\mathrm{I}}/d\Upsilon = U_{\mathrm{I}} + A_{\mathrm{I}}$. This LOC is absent for recondensation because the initial velocity of propagation, $dX_{\mathrm{I}}/d\Upsilon = A_0 + U_0$, is, as we show below, zero. We now discuss the expansion as it proceeds form $\check{X}$ to $\hat{X}$.

1.2.1 The Virtual Expansion Front at $\check{X}$ (all Υ). The only unknown quantity at the *virtual expansion front* at $\check{X}$ is $\check{U}$. To evaluate it we proceed as in [16] and conserve particles in the limit $\Upsilon = 1 + \Delta\Upsilon$. This is done in Appendix A, the overall results being

$$\check{X} = -\frac{3-\gamma}{\gamma-1}(\Upsilon - 1), \quad \text{(all } \gamma) \tag{5a}$$

$$\check{A} = 0, \quad \check{U} = -\frac{3-\gamma}{\gamma-1}. \quad \text{(all } \gamma) \tag{5b}$$

The quantity $2A/(\gamma-1)+U$ plays an important role in the theory of terminating expansions, as seen in Appendices C and D. The value at $\check{X}$ is

$$2\check{A}/(\gamma-1)+\check{U} = -(3-\gamma)/(\gamma-1). \quad \text{(all } \gamma) \tag{5c}$$

Equations (5), since they are based on a near-surface property, are valid for all γ, even $\gamma = 1$. Numerical values of $\check{U}$ are given in Table 1.

1.2.2 The Surface at $X = 0\,(\Upsilon = 1)$. Unknown quantities at the surface at $X = 0\,(\Upsilon = 1)$ include both A_0 and U_0. A particularly simple way to derive A_0 and U_0, and examine the relation $dX_{\mathrm{I}}/d\Upsilon$, is as follows. We first note that, at the moment when the expansion terminates abruptly at $\Upsilon = 1$ and recondensation sets in, the change at the surface can be regarded as occurring in two steps. First the effusing surface is sealed and we have the same situation as for reflection (Sect. 1.3):

$$A = A_0^{\mathrm{ref}} = (3-\gamma)/2, \quad U = U_0^{\mathrm{ref}} = 0 \quad (\text{all } \gamma; \Upsilon = 1) \tag{6a}$$

The sealed surface is now removed and the factor seen in (1a) is applied to A_0^{ref} giving the result,

$$A_0 = (3-\gamma)/(\gamma+1). \quad (\text{all } \gamma; \Upsilon = 1) \tag{6b}$$

The quantity U_0 now follows by analogy with (1b):

$$U_0 = -A_0 = -(3-\gamma)/(\gamma+1), \quad (\text{all } \gamma; \Upsilon = 1) \tag{6c}$$

and we see that, at the surface, the initial velocity of propagation of the disturbance $dX_{\mathrm{I}}/d\Upsilon = A_0+U_0$, is indeed zero. In making these arguments we neglect the outward movement of the surface as the recondensation proceeds. Again the quantity $2A/(\gamma-1)+U$ plays an important role as in Appendices C and D, and again the results are valid for all γ, even $\gamma = 1$. Numerical values of A_0 are given in Table 1.

Alternatively, one can derive A_0 by conserving particles in the limit $\Upsilon = 1 + \Delta\Upsilon$ (Appendices A and B).

1.2.3 Approximate Results for $X = 0$ (all Υ). We are not aware of a rigorous description valid for $X = 0$ (all Υ) other than that obtained by using the full solutions for region II with $X = 0$ (Appendices C and D). Approximate results are readily obtained, however, by noting that the following expressions satisfy the flow equations for all γ, and are exact at $X = 0$ and $\Upsilon = 1$:

$$\begin{aligned} A &\approx A_0\Upsilon^{-(\gamma-1)/2}, \quad \text{(all } \gamma) \\ U &\approx -A_0 + X\Upsilon^{-1}. \quad \text{(all } \gamma) \end{aligned} \tag{7}$$

To establish to what extent (7) is useful, we include with the tabulations of Table 3 not only exact analytical and numerical results but also values at $X = 0$ according to (7). The approximation for A, but not that for U, is seen to be acceptable. We have not yet succeeded in obtaining an approximation for P valid for $\gamma = 1$.

1.2.4 Region II (all Υ). It is region II, the "post-pulse regime" of [2], which is the fundamental obstacle to describing analytically a terminating expansion. We explored previously [16], for $\gamma = 5/3$ and conditions of *reflection*, a method pioneered by Stanyukovich [3] for resolving prob-

Table 3. Comparison of analytical, numerical, and approximate results for terminating, effusion-like expansions with $\Upsilon = 2$ and *recondensation.* The temporal and spatial steps were taken as $\Delta\Upsilon = 0.0002$ and $\Delta X = 0.00125$

γ	X	A analytical[a]	A numerical from (3)	A approx. from (7)	U analytical[a]	U numerical from (3)	U approx. from (7)
5/3	0	0.4022	0.4103	0.397	−0.3358	−0.3009	−0.5
	0.2	0.4348	0.4354	...	−0.1572	−0.1558	...
	1	0.5535	0.5541	...	0.5751	0.5767	...
	2	0.6742	0.6746	...	1.5350	1.5364	...
	2.3431 (X_{II})	0.7071	...	...	1.8787	...	...
7/5	0	0.5814	0.5855	0.580	−0.4712	−0.4637	−0.667
	0.2	0.6037	0.6063	...	−0.2800	−0.2674	...
	1	0.6847	0.6851	...	0.5015	0.5032	...
	2	0.7654	0.7657	...	1.5227	1.5245	...
	2.4756 (X_{II})	0.7937	...	...	2.0315	...	...
9/7	0	0.6785	0.6806	0.679	−0.5428	−0.5557	−0.75
	0.2	0.6953	0.6979	...	−0.3452	−0.3279	...
	1	0.7566	0.7570	...	0.4613	0.4631	...
	2	0.8173	0.8176	...	1.5125	1.5145	...
	2.5457 (X_{II})	0.8409	...	...	2.1137	...	...
11/9	0	...	0.7403	0.741	...	−0.6142	−0.8

[a] For $\gamma = 5/3$, (C6) and (C7) were used. For $\gamma = 7/5$, (D3) and (D4), as well as (A6) and (A7) of [2] were used with identical results. For $\gamma = 9/7$, (A8) and (A9) of [2] were used. Values at X_{II} are in all cases from (8)

Table 4. Explicit results for region II of terminating, effusion-like expansions with *recondensation*. X_{II}, A_{II}, and U_{II} are from (8). The temporal and spatial steps were taken as $\Delta\Upsilon = 0.0002$ and $\Delta X = 0.00125$ for $\Upsilon = 2$, and $\Delta\Upsilon = 0.0016$ and $\Delta X = 0.01$ otherwise

Υ	X	A for $\gamma = 5/3$ (analytical from App. C)	U for $\gamma = 5/3$	A for $\gamma = 7/5$ (analytical from App. D)	U for $\gamma = 7/5$	A for $\gamma = 9/7$ [numerical from (3)]	U for $\gamma = 9/7$
2	0	0.4022	−0.3358	0.5814	−0.4712	0.6806	−0.5557
	0.5	0.4815	0.1140	0.6356	0.0098	0.7198	−0.0443
	1	0.5535	0.5751	0.6847	0.5015	0.7570	0.4631
	1.5	0.6180	1.0482	0.7282	1.0051	0.7898	0.9820
	2	0.6742	1.5350	0.7654	1.5227	0.8176	1.5145
	2.3431 (X_{II})	0.7071	1.878	...	...	...	...
	2.4756 (X_{II})	...	...	0.7937	2.0315	...	...
	2.5	...	...	...	...	0.8390	2.0612
	2.5457 (X_{II})	...	...	...	...	0.8409	2.1137
4	0	0.3228	−0.2222	0.5071	−0.3307	0.6038	−0.4799
	1	0.3592	0.0982	0.5327	0.0058	0.6356	−0.0382
	2	0.3919	0.4233	0.5558	0.3467	0.6526	0.3070
	4	0.4464	1.0883	0.5939	1.0423	0.6818	1.0196
	6	0.4844	1.7766	0.6200	1.7598	0.7017	1.7528
	8 (X_{II})	0.5	2.5	...	...	...	...
	8	...	...	0.6312	2.5071	0.7102	2.5119
	8.8809 (X_{II})	...	...	0.6300	2.8502	...	...
	9	...	...	...	...	0.7085	2.9002
	9.3726 (X_{II})	...	...	...	...	0.7071	3.0503
8	0	0.2528	−0.1451	0.4422	−0.2315	0.5358	−0.4225
	2	0.2808	0.1372	0.4584	0.0618	0.5665	−0.0017
	4	0.3007	0.4222	0.4730	0.3574	0.5810	0.3219
	8	0.3333	1	0.4967	0.9560	0.5991	0.9305
	12	0.3558	1.5896	0.5129	1.5654	0.6117	1.5515
	16	0.3660	2.1947	0.5206	2.1881	0.6177	2.1845
	20	0.3578	2.8263	0.5177	2.8290	0.6161	2.8329
	20.6863 (X_{II})	0.3536	2.9393	...	...	...	...
	22	...	...	0.5111	3.1594	0.6118	3.1646
	24 (X_{II})	...	...	0.5	3.5	...	...
	24	...	...	...	...	0.6046	3.5024
	25.9454 (X_{II})	...	...	...	...	0.5946	3.8378

lems such as that of region II. This is reconsidered for $\gamma = 5/3$ in Appendix C and for $\gamma = 7/5$ in Appendix D, in both cases under conditions of *recondensation*. The case $\gamma = 9/7$ is discussed in [2]. Various analytical, numerical [30, 31], and approximate results are compared, with favorable outcome, in Table 3.

It is important to note that the analytical results, both here and in [2], imply the existence of a virtual region from $\check{X}$ to $X = 0$, whereas the numerical results such as those of Table 3 were based on equating A to zero "one spatial step" behind the surface. This might seem to alter, perhaps unacceptably, the details of how one conserves particles in the limit $\Upsilon = 1 + \Delta\Upsilon$, as in Appendix A. Conservation of particles is therefore reconsidered in Appendix B in a way which is compatible with equating A to zero "one spatial step" behind the surface. The same values of A_0 and U_0 are obtained, showing that the analytical and numerical approaches are indeed equivalent.

We chose not to derive general analytical solutions for $\gamma = 9/7$, 11/9, and 1 because of the extreme complexity of the problems. Instead, numerical results were obtained as in Tables 4 and 5.

1.2.5 The Second LOC *at* X_{II} *(all* Υ*).* Region II terminates with an abrupt change of slope at the second LOC at X_{II} governed by $dX_{\text{II}}/d\Upsilon = U_{\text{II}} + A_{\text{II}}$. In view of (1c) and (1d) we therefore have for $\gamma \neq 1$

$$X_{\text{II}} = \frac{\gamma+1}{\gamma-1}\left(\Upsilon - \Upsilon^{(3-\gamma)/(\gamma+1)}\right), \qquad (\gamma \neq 1) \tag{8a}$$

$$A_{\text{II}} = \Upsilon^{-2(\gamma-1)/(\gamma+1)}, \qquad (\gamma \neq 1) \tag{8b}$$

$$U_{\text{II}} = \frac{\gamma+1}{\gamma-1} - \frac{2}{\gamma-1}\Upsilon^{-2(\gamma-1)/(\gamma+1)} \qquad (\gamma \neq 1) \tag{8c}$$

$$2A_{\text{II}}/(\gamma-1) + U_{\text{II}} = (\gamma+1)/(\gamma-1). \qquad (\gamma \neq 1) \tag{8d}$$

Equations (8), being based on (1c) and (1d), are valid for all γ except $\gamma = 1$. U_{II} is shown in Fig. 3. (For problems connected with U_{II} in [6], see Appendix F.)

For $\gamma = 1$ the velocity of the second LOC is again $dX_{\text{II}}/d\Upsilon = U_{\text{II}} + A_{\text{II}}$, but in view of (1d) and (2a) we now have

$$X_{\text{II}} = 2\Upsilon \ln \Upsilon, \qquad (\gamma = 1) \tag{9a}$$

$$A_{\text{II}} = 1, \quad P_{\text{II}} = \Upsilon^{-2}, \qquad (\gamma = 1) \tag{9b}$$

$$U_{\text{II}} = 1 + 2\ln\Upsilon. \qquad (\gamma = 1) \tag{9c}$$

1.2.6 Region III and the Real Expansion Front at $\hat{X}$ *(all* Υ*).* Region III, the "simple expansion regime" of [2] or "flow phase" of [6], is the remanent of the release process described by (1c) or (2a) and (1d). It begins at X_{II} as in

Table 5. Continuation of explicit results for region II of expansions with *recondensation*. X_{II}, A_{II}, and U_{II} are from (8) and (9). For $\gamma = 1$ we list $P = \varrho/\varrho_K$ instead of $A = a/u_K = 1$. The temporal and spatial steps were as in Table 4

Υ	X	A for $\gamma = 11/9$ [numerical from (3)]	U for $\gamma = 11/9$	P for $\gamma = 1$ [numerical from (4)]	U for $\gamma = 1$
2	0	0.7403	−0.6142	0.0622	−0.8703
	0.5	0.7723	−0.0789	0.0887	−0.2261
	1	0.8022	0.4378	0.1201	0.3279
	1.5	0.8285	0.9659	0.1569	0.8922
	2	0.8508	1.5072	0.1964	1.4682
	2.5	0.8680	2.0636	0.2337	2.0574
	2.5890 (X_{II})	0.8706	2.1650	...	...
	2.7	...	...	0.2454	2.2985
	2.7726 (X_{II})	...	...	0.25	2.3863
4	0	0.6733	−0.5465	0.0248	−0.8634
	1	0.7004	−0.0737	0.0348	−0.2476
	2	0.7144	0.2793	0.0415	0.1585
	4	0.7380	1.0015	0.0527	0.9162
	6	0.7541	1.7438	0.0621	1.6997
	8	0.7612	2.5107	0.0675	2.4978
	9.6857 (X_{II})	0.7579	3.1793	...	...
	10	...	...	0.0661	3.3181
	11.0904 (X_{II})	...	...	0.0625	3.7726
8	0	0.6128	−0.4953	0.0101	−0.8682
	2	0.6391	−0.0426	0.0141	−0.2597
	4	0.6518	0.2938	0.0168	0.1390
	6	0.6600	0.6031	0.0189	0.4946
	8	0.6668	0.9124	0.0205	0.8298
	12	0.6771	1.5402	0.0228	1.4836
	16	0.6822	2.1793	0.0242	2.1491
	20	0.6813	2.8325	0.0244	2.8242
	24	0.6731	3.5043	0.0231	3.5106
	27.2197 (X_{II})	0.6598	4.0622	...	...
	28	...	...	0.0205	4.2109
	32	...	...	0.0168	4.9251
	33.2711 (X_{II})	...	...	0.0156	5.1589

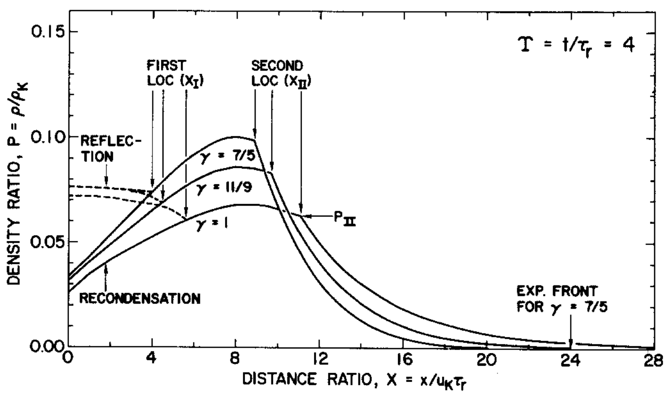

Fig. 4. Density *vs* distance for three values of γ and $\Upsilon = 4$. The branching at the left of each curve corresponds to conditions of reflection (upper branch, *dashed*) and recondensation (lower branch, *solid*). It will be noted that the density profile varies only weakly with γ. The information is numerical up to X_{II} and analytical beyond X_{II}

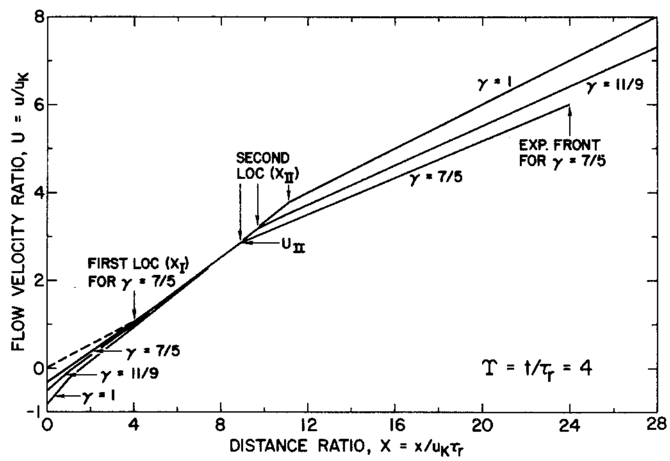

Fig. 5. Flow velocity *vs* distance for three values of γ and $\Upsilon = 4$. The branching at the left of the profile for $\gamma = 7/5$ again corresponds to conditions of reflection (upper branch, *dashed*) and recondensation (lower branch, *solid*). It will be noted that the flow velocity profile varies even more weakly with γ than does the density profile. The information is numerical up to X_{II} and analytical beyond X_{II}

(8a) or (9a), and terminates at the *real expansion front* at $\hat{X}$, described for all γ by

$$\hat{X} = \frac{\gamma+1}{\gamma-1}\Upsilon, \quad \text{(all } \gamma) \tag{10a}$$

$$\hat{A} = \hat{P} = 0, \quad \hat{U} = \frac{\gamma+1}{\gamma-1}. \quad \text{(all } \gamma) \tag{10b}$$

As already pointed out by [2], for $\gamma = 1$ both $\hat{X}$ and $\hat{U}$ tend to infinity.

Tables 4 and 5 give results for region II under conditions of recondensation, while Figs. 4 to 7 show examples of the variation of P and U with X. Other information of this type is given in [2,4,6,16]. (Note that Fig. 4c of [4] has

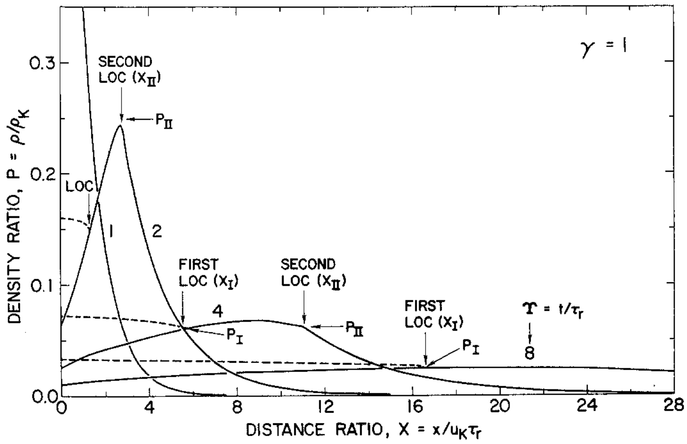

Fig. 6. Density *vs* distance for $\gamma = 1$ and four values of Υ. The branching at the left of each curve corresponds to conditions of reflection (upper branch, *dashed*) and recondensation (lower branch, *solid*). The information is numerical up to X_{II} and analytical beyond X_{II}

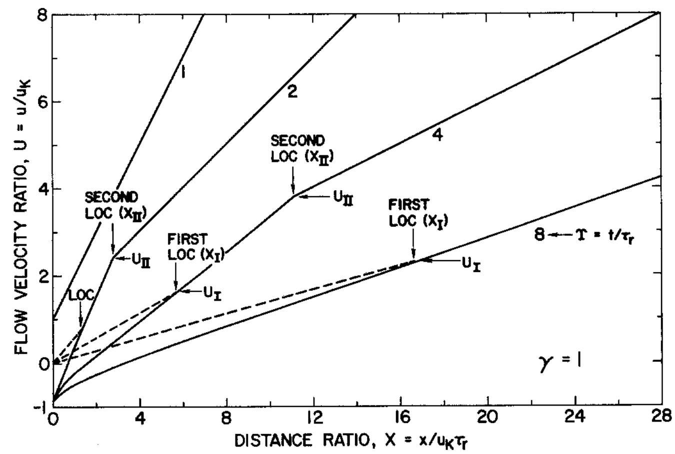

Fig. 7. Flow velocity *vs* distance for $\gamma = 1$ and four values of Υ. The branching at the left of the profile for $\Upsilon = 2$ again corresponds to conditions of reflection (upper branch, *dashed*) and recondensation (lower branch, *solid*). The information is numerical up to X_{II} and analytical beyond X_{II}

a surface boundary condition differing from that of (6). This is because it was attempted to take into account the recondensation Knudsen layer [28, 29].) An important aspect of the solutions, evident in Figs. 4 and 5, is that P and U for a given Υ are roughly independent of γ, a situation not previously recognized. Analysis of information as in Fig. 1, where the emitted particles have a range of masses [18, 19], should be correspondingly facilitated. Table 8 summarizes the availability of analytical solutions, approximate forms, and tabulations.

1.3 Results for a Terminating, Effusion-Like Expansion with Reflection

At the moment that an effusion-like expansion terminates, and conditions of *reflection* apply, there is again an abrupt change of boundary conditions at the effusing surface. U falls from 1 to 0, and A falls from 1 to a still undetermined value A_0^{ref} (identical to the quantity L of [16]). As a result the expansion evolves from that described by (1c) and (1d) to one with three parts beginning at the surface (Fig. 3). These will be termed *region I* (the "reflection regime" of [2]), *region II* and *region III*. The regions are separated by two LOC's at X_I and X_{II}, and we note that the part of region II lying beyond the first LOC at X_I, as well as the entirety of region III are identical to what is applicable under conditions of *recondensation* (Sect. 1.2).

1.3.1 The Surface at $X = 0\,(\Upsilon = 1)$. At the moment when the expansion terminates abruptly at $\Upsilon = 1$ and reflection sets in, the change at the surface involves simply a sealing as in Fig. 2b. U and A therefore change to

$$A = A_0^{\text{ref}}, \quad U = U_0^{\text{ref}} = 0. \quad (\text{all } \gamma; \Upsilon = 1) \qquad (11\text{a})$$

Since (11a) already satisfies the flow equations, the quantity A_0^{ref} is not determined at this point. Rather, it is necessary to conserve particles in the limit $\Upsilon = 1 + \Delta\Upsilon$ [16], the result being

$$A_0^{\text{ref}} = (3-\gamma)/2, \quad (\text{all } \gamma) \qquad (11\text{b})$$

$$2A_0^{\text{ref}}/(\gamma-1) + U_0^{\text{ref}} = (3-\gamma)/(\gamma-1), \quad (\text{all } \gamma) \qquad (11\text{c})$$

with representative values as in Table 1. Equations (11b) and (11c), since they are based on a near-surface property, are valid for all γ, even $\gamma = 1$.

1.3.2 Region I for $\gamma = 5/3$ (all Υ). We have already shown [16] that the first part of the expansion ("region I") is described for $\gamma = 5/3$ by the remarkably simple relations:

$$A = A_0^{\text{ref}}\Upsilon^{-(\gamma-1)/2}, \quad U = X\Upsilon^{-1}, \quad (\gamma = 5/3) \qquad (12)$$

results which are easily shown to satisfy the flow equations, the conditions at $X = 0$, and the LOC which terminates region I at X_I.

1.3.3 The first LOC *at X_I for $\gamma = 5/3$ (all Υ).* Region I terminates with an abrupt change of slope at the first LOC at X_I, governed by $dX_I/d\Upsilon = U_I + A_I$. In view of (12) we therefore have for $\gamma = 5/3$

$$X_I = [(3-\gamma)/(\gamma-1)](\Upsilon - \Upsilon^{(3-\gamma)/2}), \quad (\gamma = 5/3) \qquad (13\text{a})$$

$$A_I = A_0^{\text{ref}}\Upsilon^{-(\gamma-1)/2}, \quad U_I = X_I\Upsilon^{-1}, \quad (\gamma = 5/3) \qquad (13\text{b})$$

$$2A_I/(\gamma-1) + U_I = (3-\gamma)(\gamma-1). \quad (\text{all } \gamma) \qquad (13\text{c})$$

U_I is shown in Fig. 3. We have taken (13c) as being generally valid, in agreement with (20a) and (43) of [2], since it can be justified as a near-surface property. (For problems connected with closely related equations in [6], see Appendix F.)

1.3.4 Approximate Results for Region I *and X_I (all Υ).* As will be discussed in Appendix E, (12) and (13) are rigorously valid only for $\gamma = 5/3$. Nevertheless, they satisfy the flow equations for all γ, and are exact at $X = 0$ and $\Upsilon = 1$. Only the boundary condition at X_I is violated for $\gamma < 5/3$, as is discussed in Appendix E. One might therefore expect the equations, which have a remarkably simple form, to be generally applicable provided small errors can be tolerated.

To establish to what extent (12) and (13) are generally useful, we include with the tabulations of Tables 6 and 7 not only exact analytical and numerical results but also values at

Table 6. Explicit results for region I of terminating, effusion-like expansions with *reflection*. Unmarked values are exact and those marked "simple" or "s" are approximate forms from (14)

Υ	X	A for $\gamma=5/3$ (analytical)[a]	U for $\gamma=5/3$	A for $\gamma=7/5$ (analytical)[a]	U for $\gamma=7/5$	A for $\gamma=9/7$ (analytical)[a]	U for $\gamma=9/7$
2	0 (rigorous)	0.5291	0	0.6908	0	0.7695	0
	0 (simple)	0.5291	0	0.696	0	0.776	0
	0.5	0.5291	0.25	0.6905	0.2628	0.7690	0.3095
	0.8252 (X_I)	0.5291	0.4126	...	...	...	...
	1	...	...	0.6896	0.5257	0.7679	0.5802
	1.0515 (X_I)	...	...	0.6895	0.5527	...	...
	1.036 (X_I, s)	...	...	0.696	0.518	...	...
	1.1603 (X_I)	...	...	...	...	0.7675	0.6558
	1.131 (X_I, s)	...	...	...	...	0.776	0.566
4	0 (rigorous)	0.4200	0	0.5977	0	0.6921	0
	0 (simple)	0.4200	0	0.606	0	0.703	0
	1	0.4200	0.25	0.5974	0.2597	0.6918	0.2954
	2	0.4200	0.5	0.5966	0.5196	0.6909	0.5567
	2.9603 (X_I)	0.4200	0.7401	...	...	...	...
	3	...	...	0.5953	0.7796	0.6897	0.7699
	3.9730 (X_I)	...	...	0.5934	1.0328	...	...
	3.874 (X_I, s)	...	...	0.606	0.969	...	...
	4	...	...	...	...	0.6885	0.9399
	4.5004 (X_I)	...	...	...	...	0.6880	1.0119
	4.312 (X_I, s)	...	...	...	...	0.703	1.078
8	0 (rigorous)	0.3333	0	0.5179	0	0.6235	0
	0 (simple)	0.3333	0	0.528	0	0.637	0
	2	0.3333	0.25	0.5176	0.2574	0.6232	0.2849
	4	0.3333	0.5	0.5169	0.5149	0.6224	0.5387
	6	0.3333	0.75	0.5158	0.7725	0.6215	0.7481
	8 (X_I)	0.3333	1	...	...	...	...
	8	...	...	0.5142	1.0303	0.6205	0.9165
	10	...	...	0.5120	1.2884	0.6195	1.0530
	11.2341 (X_I)	...	...	0.5104	1.4478	...	...
	10.888 (X_I, s)	...	...	0.528	1.361	...	...
	12	...	...	...	...	0.6186	1.1658
	13.0268 (X_I)	...	...	...	...	0.6182	1.2166
	12.336 (X_I, s)	...	...	...	...	0.637	1.542

[a] For $\gamma = 5/3$, (12) and (13) were used. For $\gamma = 7/5$, (A10) and (A11) of [2] were used for $X < X_I$, and the present (D5) and (D6) for $X = X_I$. For $\gamma = 9/7$, (A14–A17) of [2] were used

$X = 0$ and X_I according to (12) and (13) (marked "simple" or "s"). There is seen to be agreement to within 6% and, for this reason, we propose that (12) and (13) rather than exact analytical or numerical solutions be used for $\gamma < 5/3$:

$$X_I \approx [(3-\gamma)/(\gamma-1)](\Upsilon - \Upsilon^{(3-\gamma)/2}), \quad (\gamma \neq 1) \tag{14a}$$

$$A \approx A_I \approx A_0^{\text{ref}} \Upsilon^{-(\gamma-1)/2}, \quad (\text{all } \gamma) \tag{14b}$$

$$U \approx X\Upsilon^{-1}, \quad U_I \approx X_I \Upsilon^{-1}. \quad (\text{all } \gamma) \tag{14c}$$

For some purposes it may be useful, notwithstanding the obvious simplicity of (14), to have exact expressions for X_I, A_I, and U_I. For $\gamma = 7/5$ they can be obtained by introducing $5A + U = 4$ into (D3) and (D4) with results as in (D5) and (D6). For $\gamma = 9/7$ one substitutes $7A + U = 6$ into (A16) and (A17) of [2]. (These results, it might be noted, constitute a simplification of (A12), (A13), (A16), and (A17) of [2]. The latter equations are, however, otherwise correct.)

Equations (14) are not all useful for $\gamma = 1$ and we now indicate the corresponding approximate forms. For A and U we have, in accordance with (2a) and (14b),

$$A = A_I = 1, \quad (\gamma = 1) \tag{15a}$$

$$U \approx X\Upsilon^{-1}, \quad U_I \approx X_I \Upsilon^{-1}. \quad (\text{all } \gamma) \tag{15b}$$

the latter expression being best justified numerically (Table 7). By substituting (15b) into (4b) we obtain

$$P \approx P_I \approx P_0 \Upsilon^{-1}. \quad (\text{all } \gamma) \tag{15c}$$

The first LOC at X_I is again governed by $dX_I/d\Upsilon = U_I + A_I$, but in view of (15a) and (15b) we now have

$$X_I \approx \Upsilon \ln \Upsilon, \quad U_I \approx \ln \Upsilon. \quad (\gamma = 1) \tag{16}$$

Finally $P_0^{\gamma=1}$, applying specifically for $\gamma = 1$, is evaluated by conserving particles in the limit $\Upsilon = 1 + \Delta\Upsilon$. The quantity in region I is just $Q_I = PX_I$, that in region II is $Q_{II} = P(X_{II} - X_I) + \frac{1}{2}(1-P)(X_{II} - X_I)$, and that in region III has the value $Q_{III} = \Upsilon^{-1}$ seen in (A1). The condition $Q_I + Q_{II} + Q_{III} = 1$ finally yields

$$P_0^{\gamma=1} \approx 1/3. \quad (\gamma = 1) \tag{16c}$$

1.3.5 Region II *and the Second* LOC *at* X_{II} *(all* Υ*).* With regard to $\gamma = 5/3$ and $7/5$, we note that the solutions discussed in Sect. 1.2 for region II and here reproduced in Appendices C and D apply equally under conditions of recondensation and reflection. This is because region II lies *beyond* X_I and "knows nothing" about the existence of the first LOC in those instances where there is one. Thus we have the following inequality:

$$X_{II} > X_I. \quad (\text{all } \gamma)$$

The solutions are valid from X_I to X_{II}.

Table 7. Continuation of explicit results for region I of expansions with *reflection.* Unmarked results are exact and those marked "simple" or "s" are approximate forms from (14) and (16). The temporal and spatial steps were taken as $\Delta\Upsilon = 0.0016$ and $\Delta X = 0.01$

Υ	X	A for $\gamma = 11/9$ [numerical from (3)]	U for $\gamma = 11/9$	P for $\gamma = 1$ [numerical from (4)]	U for $\gamma = 1$
2	0 (rigorous)	0.8164	0	0.1598	0
	0 (simple)	0.823	0	0.167	0
	0.5	0.8159	0.2757	0.1587	0.2956
	1	0.8133	0.5291	0.1567	0.5630
	1.186 (X_{I}, s)	0.823	0.593	...	...
	1.386 (X_{I}, s)	...	...	0.167	0.693
4	0 (rigorous)	0.7512	0	0.0719	0
	0 (simple)	0.762	0	0.0833	0
	1	0.7509	0.2715	0.0716	0.2875
	2	0.7501	0.5404	0.0708	0.5722
	3	0.7489	0.8122	0.0694	0.8569
	4	0.7461	1.066	0.0676	1.142
	4.568 (X_{I}, s)	0.762	1.142	...	...
	5	...	...	0.0649	1.436
	5.545 (X_{I}, s)	...	...	0.0833	1.386
8	0 (rigorous)	0.6919	0	0.0329	0
	0 (simple)	0.706	0	0.0417	0
	2	0.6917	0.2664	0.0328	0.2807
	4	0.6910	0.5315	0.0325	0.5600
	6	0.6898	0.7968	0.0320	0.8394
	8	0.6882	1.062	0.0312	1.119
	10	0.6858	1.331	0.0303	1.399
	12	0.6825	1.582	0.0293	1.679
	13.20 (X_{I}, s)	0.706	1.650	...	...
	14	...	...	0.0280	1.959
	16	...	...	0.0265	2.232
	16.64 (X_{I}, s)	...	...	0.0417	2.079

Table 8. Overview of the availability of analytical solutions, approximate forms, and tabulations for terminating expansions

	Recondensation (region II only)			Reflection (region I only)		
γ	Analytical solutions	Approx. forms	Tabulations	Analytical solutions	Approx. forms	Tabulations
5/3	App. C	(7)	Table 4	(12, 13)	...	Table 6
7/5	App. D	(7)	Table 4	[2]	(14)	Table 6
9/7	[2]	(7)	Table 4	[2]	(14)	Table 6
11/9	...	(7)	Table 5	...	(14)	Table 7
1	[2]	...	Table 5	...	(15, 16)	Table 7

1.3.6 Region III *and the Real Expansion Front at* $\hat{X}$ *(all* Υ*).* Region III requires no comment, as it is exactly the same for all surface conditons in the sense that it begins at X_{II} as in (8a) or (9a), is described by (1c) or (2a) and (1d), and terminates at $\hat{X}$ as in (10a).

Tables 6 and 7 give results for region I under conditions of reflection. Also Figs. 4 to 7 are relevant to conditions of reflection, with region I represented by the dashed portions. The availability of analytical solutions, approximate forms, and tabulations is summarized in Table 8.

2 Discussion

We have considered terminating, effusion-like expansions as are relevant when gases are released from a pulsed nozzle or when solids are sputtered with intense laser pulses, a subject treated previously in [2, 6, 16]. We recognize that some of the results appear in [2, 6, 16] but justify the present work on the basis that we have used what we feel to be simpler mathematical methods. Furthermore, we have supplemented the analytical solutions both with approximations and numerical results.

We found that one of the biggest uncertainties in obtaining analytical solutions was to be convinced of the correctness of the changes of boundary conditions at the surface at $X = 0$ when the expansions terminate abruptly at $\Upsilon = 1$. It should be recalled, in this regard, that the relation appropriate to *reflection*,

$$A_0^{\mathrm{ref}} = (3-\gamma)/2\,, \qquad (\text{all } \gamma) \tag{11b}$$

satisfies the flow equations for all A_0^{ref} and it is therefore non-trivial to deduce the correct A_0^{ref}. Indeed, a value correct only for $\gamma = 5/3$, namely $(\gamma+1)/4$, was proposed in [6] (Appendix F). Also the idea, when there is *recondensation*, of making the changes in two steps so as to obtain the result,

$$A_0 = (3-\gamma)/(\gamma+1)\,, \qquad (\text{all } \gamma; \Upsilon = 1) \tag{6b}$$

may possibly be naive. Nevertheless, our analytical values of A_0^{ref} and A_0 agree fully with those of [2] and, in addition, have been tested numerically. For example, for $\gamma = 7/5$

the numerical value of A_0^{ref} was 0.80005 (instead of the analytical value 0.8) and of A_0 was 0.688 (instead of 0.667). If A_0^{ref} is taken as $(\gamma+1)/4$ then we obtain for $\gamma = 7/5$ the unacceptable analytical values $A_0^{\mathrm{ref}} = 0.6$ and $A_0 = 0.5$. Nevertheless, the surface conditions used both here and in [2] for recondensation are wrong in so far as they do not take into account the *recondensation Knudsen layer* [28,29].

It was noted that the remarkably simple relations for region I valid for $\gamma = 5/3$ and conditions of *reflection* (12, 13), if used for γ other than 5/3, gave results which differed only slightly from more rigorous results. For example, A for $X = 0$ is obtained to within 2% (Tables 6 and 7). Simple relations can also be constructed for $\gamma = 1$ (15, 16). The approximations amount to requiring that A or P retain, for $X > 0$, the values appropriate to $X = 0$ and that U is always given by $U \approx X\Upsilon^{-1}$. The failure of (12–16) to be exact for γ other than 5/3 is discussed in Appendix E.

Simple relations for $X = 0$, valid under conditons of *recondensation*, are also readily devised as in (7). Only that for A is useful, however, agreeing with the more rigorous results generally to within 2% (Tables 4 and 5).

Table 3 serves to compare the analytical, numerical, and approximate solutions for region II when there is *recondensation*. The agreement is in all cases rather good and a possible conclusion is that the various analytical solutions [2, 6, 16] are correct. From another point of view the numerical solutions, obtained using the methods of Godunov and Lax-Wendroff with time-varying mesh [30, 31], are seen to be acceptable. That there should be doubt in either case rests mainly with the somewhat different approach used to describe the surface at $X = 0$ under conditions of recondensation. Thus the analytical solutions imply the existence of a virtual region from $\check{X}$ to $X = 0$, whereas the numerical results are based on equating A to zero "one spatial step" behind the surface.

As overall conclusions we wish to indicate the following:

(a) At least four types of terminating expansion can be envisaged, as outlined in Table 2.

(b) When an expansion terminates and there is *recondensation*, U falls abruptly from 1 to $-A_0$, and A from 1 to A_0, with A_0 given by $(3-\gamma)/(\gamma+1)$. As time increases, the solutions evolve into two well-defined regions, here designated II and III. Region II begins at the virtual expansion front at $\check{X}$, while region III terminates at the real expansion front at $\hat{X}$ (Fig. 3).

(c) When an expansion terminates and there is *reflection*, U falls abruptly from 1 to 0, and A from 1 to A_0^{ref}, with A_0^{ref} given by $(3-\gamma)/2$. As time increases, the solutions are now more complex as they evolve into three regions, here designated I, II, and III. Region I begins at the effusing surface at $X = 0$, while region III again terminates at the real expansion front at $\hat{X}$ (Fig. 3).

(d) An important simplification is that the solutions for region II and III are the same no matter what are the surface conditions. This is because the different surface conditions affect only region I and the other regions lie beyond region I. In effect the inequality $X_{\mathrm{II}} > X_{\mathrm{I}}$ holds for all γ.

(e) Another simplification is that plots of ϱ versus x and u versus x are roughly independent of γ, thence of the nature of the sputtered particles (Figs. 4 and 5).

(f) The somewhat complicated analytical solutions for region II under conditions of *recondensation* (Appendices C and D) can be approximated at $X = 0$ by the remarkably simple forms seen in (7). These forms satisfy the flow equations, and are exact at $X = 0$ and $\Upsilon = 1$, but only that for A is useful:

$$A \approx A_0\Upsilon^{-(\gamma-1)/2}, \quad (\text{all } \gamma)$$
$$U \approx -A_0 + X\Upsilon^{-1}. \quad (\text{all } \gamma) \tag{7}$$

(g) Simple forms as in (12–16) can be devised also for conditions of *reflection*. They are valid for all of region I from $X = 0$ to X_{I}, satisfy the flow equations, and are exact at $X = 0$ and $\Upsilon = 1$:

$$A \approx A_0^{\mathrm{ref}}\Upsilon^{-(\gamma-1)/2}, \quad U \approx X\Upsilon^{-1}, \quad (\text{all } \gamma)$$
$$P \approx \frac{1}{3}\Upsilon^{-1}, \quad U \approx X\Upsilon^{-1}. \quad (\gamma = 1) \tag{14}$$

(h) The availability of analytical solutions, approximate forms, and tabulations is summarized in Table 8.

Acknowledgements. We note with pleasure that there was an extensive exchange of information with Herbert Urbassek (Universität Kaiserslautern, W-6750 Kaiserslautern, Germany). For example, he evaluated independently of us (A6–A9) of [2] as used in Table 3.

This work was made possible by the generous support of the Istituto per la Ricerca Scientifica e Tecnologica (IRST) and of the Dipart. di Fisica dell'Univ. di Trento, which together made possible extended visits by one of the authors (RK) to Trento in February and again in September, 1992.

Appendix A

Evaluation of $\check{U}$, A_0, and U_0 with Virtual Region

We here evaluate $\check{U}$, A_0, and U_0 under conditions of *recondensation* by conserving the number of particles for a time near $\Upsilon = 1$, namely $\Upsilon = 1 + \Delta\Upsilon$, when A for region II is rigorously linear both to the "left" and to the "right" of the effusing surface. To the "left", i.e. in the *virtual region*, Q_{II} has a contribution

$$Q_{\mathrm{II}}^{\mathrm{l}} = \int_0^{-\check{U}\Delta\Upsilon} \left(\frac{\Delta A}{\Delta X}X\right)^{2/(\gamma-1)} dX = \int_0^{-\check{U}\Delta\Upsilon} \left(\frac{A_0}{-\check{U}\Delta\Upsilon}X\right)^{2/(\gamma-1)} \mathrm{d}X = -\left(A_0^{(\gamma+1)/(\gamma-1)}\right)\frac{\gamma-1}{\gamma+1}\frac{\check{U}\Delta\Upsilon}{A_0},$$

where we note that $\check{U}$ is negative. To the "right" Q_{II} has a contribution

$$Q_{\mathrm{II}}^{\mathrm{r}} = \int_0^{X_{\mathrm{II}}} \left(A_0 + \frac{\Delta A}{\Delta X}X\right)^{2/(\gamma-1)} dX = \int_0^{2\Delta\Upsilon} \left(A_0 + \frac{1-A_0}{2\Delta\Upsilon}X\right)^{2/(\gamma-1)} \mathrm{d}X = \left(1 - A_0^{(\gamma+1)/(\gamma-1)}\right)\frac{\gamma-1}{\gamma+1}\frac{2\Delta\Upsilon}{1-A_0}.$$

Finally, the region from X_{II} to $\hat{X}$ is the same as when there is reflection [16]:

$$Q_{\mathrm{III}} = \int_{X_{\mathrm{II}}}^{\hat{X}} A^{2/(\gamma-1)} dX = \Upsilon^{-1} = 1 - \Delta\Upsilon \,. \tag{A1}$$

By requiring conservation of particles, $Q_{\mathrm{II}}^{\mathrm{l}} + Q_{\mathrm{II}}^{\mathrm{r}} + Q_{\mathrm{III}} = 1$, it follows without difficulty that A_0 and $\check{U}$ are given by

$$A_0 = (3-\gamma)/(\gamma+1) \,, \tag{A2}$$

$$\check{U} = -2A_0/(1-A_0) = -(3-\gamma)/(\gamma-1) \,. \tag{A3}$$

Note that (A3) can also be obtained by equating the slopes, $\Delta A/\Delta X$, to the "left" and to the "right" of the surface. Similarly, by equating $\Delta U/\Delta X$ to the "left" and "right", one obtains

$$U_0 = -A_0 \,. \tag{A4}$$

We take these results as showing that, in resolving Ψ as in Appendices C and D there is no separate information contained in A_0 and U_0. Indeed, if this assumption is not made the number of conditions exceeds the number of unknowns. We note also that if the slopes to the "left" do not equal those to the "right", then there would be a LOC at the surface, but there is no such LOC under coditions of recondensation.

Appendix B

Evaluation of A_0 and U_0 without Virtual Region.

We here evaluate A_0 and U_0 under conditions of *recondensation* by conserving the number of particles for a time near $\Upsilon = 1$, namely $\Upsilon = 1 + \Delta\Upsilon$, when A for region II is rigorously linear to the "right" of the effusing surface, while instead of a virtual region to the "left" we allow for a recondensing flux. This approach lies at the basis of the numerical method used for the various tabulations.

We now have, instead of $Q_{\mathrm{II}}^{\mathrm{l}}$ of Appendix A, the recondensed quantity, $Q_{\mathrm{II}}^{\mathrm{rec}}$:

$$Q_{\mathrm{II}}^{\mathrm{rec}} = -U_0 A_0^{2/(\gamma-1)} \Delta\Upsilon \,. \tag{B1}$$

$Q_{\mathrm{II}}^{\mathrm{r}}$ and Q_{III} remain the same and the final results are

$$A_0 = (3-\gamma)/(\gamma+1) \,, \tag{B2}$$

$$U_0 = -A_0 \,. \tag{B3}$$

The description of the recondensation problem is thus the same whether or not a virtual region is assumed and we are therefore not surprised that the analytical results (for which a virtual region is implied) agree with the numerical results [described by (B1)] in Table 3.

Appendix C

Solutions for Region II *for $\gamma = 5/3$ under Conditions of Recondensation*

The resolution of region II has already been discussed [16] for conditions of *reflection* and is now reconsidered as modified for *recondensation.* Without going into detail we will argue here simply that the flow equations (3) can be transformed to the following:

$$\frac{3-\gamma}{(\gamma-1)A}\frac{\partial\Psi}{\partial A} - \left(\frac{2}{\gamma-1}\right)^2 \frac{\partial^2\Psi}{\partial U^2} + \frac{\partial^2\Psi}{\partial A^2} = 0 \,, \quad \text{(continuity equation)} \tag{C1}$$

$$\frac{2A\Upsilon}{\gamma-1} = \frac{\partial\Psi}{\partial A} \,, \quad \text{(Euler equation)} \tag{C2}$$

$$X = U\Upsilon - \partial\Psi/\partial U \,. \quad \text{(an Ansatz)} \tag{C3}$$

Equation (C1) is satisfied for $\gamma = 5/3$ by

$$\Psi = \frac{F(3A+U)}{A} = \sum \frac{C_n(3A+U)^n}{A} \,, \tag{C4}$$

as is easily shown by substitution into (C1). The fact that the same result will be obtained proves that region II for $\gamma = 5/3$ is independent of the surface conditions. As already noted in Sect. 1.3 this result is not surprising in view of the inequality, valid for $\gamma > 1$,

$$X_{\mathrm{II}} > X_{\mathrm{I}} \,.$$

The constants C_n can be deduced by evaluating (C2) and (C3) in terms of (C4) at $\check{X}$ and X_{II}. As seen in Table 9 this gives four conditions and we therefore need four constants. Furthermore, since (C2) and (C4) together give $3AF' - F = 3A^3\Upsilon$, we choose $n = 3$ and the constants become C_0, C_1, C_2, and C_3. It is easily shown that the values $C_3 = 1/36$, $C_2 = 0$, $C_1 = -1/3$, and $C_0 = -4/9$ (the same as those proposed in [16]) satisfy the four conditions and the expression for $F(3A+U)$ is therefore

$$F(3A+U) = (3A+U)^3/36 - (3A+U)/3 - 4/9 \,. \tag{C5}$$

Table 9. Quantities used for evaluating the constants C_n for $\gamma = 5/3$ and 7/5 in Appendices C and D

γ	Position	$2A/(\gamma-1)+U$	Conditions from (C2)	Conditions from (C3)
5/3	$\check{X}$, all Υ	-2 (5c)	$F(-2)=0$	$F'(-2)=0$
	$X=0$, $\Upsilon=1$	1 (6b, 6c)	$F(1)=-3/4$	$F'(1)=-1/4$
	X_{I}, all Υ	1 (13c)	$F(2)=-8/9$	$F'(2)=0$
	X_{II}, all Υ	4 (8d)	$F(4)=0$	$F'(4)=1$
7/5	$\check{X}$, all Υ	-4 (5c)	$F(-4)=0$	$F'(-4)=F''(-4)=0$
	$X=0$, $\Upsilon=1$	8/3 (6b, 6c)	$F(\frac{8}{3})-\frac{20}{9}F'(\frac{8}{3})=\frac{1600}{729}$	$\frac{3}{10}F'(\frac{8}{3})-F''(\frac{8}{3})=\frac{8}{27}$
	X_{I}, all Υ	4 (13c)	$F(4)\approx\frac{1024}{375}$	$F'(4)\approx F''(4)\approx 0$
	X_{II}, all Υ	6 (8d)	$F(6)=0$	$F'(6)=0$, $F''(6)=1$

There is no additional information at $X = 0(\Upsilon = 1)$, as is not surprising since the values of A and U at this point are linear interpolations of those for $\check{X}$ and X_{II} (Appendix A). As an unexpected bonus, however, we find that the same set of four constants describes the simple form of X_{I} seen in (13) (Table 9 and Appendix E).

The actual solutions are as follows. From $X = U\Upsilon - \partial\Psi/\partial U$, with Ψ as in (C4), one obtains

$$12AX - 12AU\Upsilon = -(3A+U)^2 + 4 . \qquad \text{(C6)}$$

From $3A\Upsilon = \partial\Psi/\partial A$ one obtains

$$108A^3\Upsilon = -(3A+U)^3 + 9A(3A+U)^2 + 12U + 16 . \qquad \text{(C7)}$$

Equations (C6) and (C7) are easily checked by noting that they behave as required at $\check{X}$, $X = 0(\Upsilon = 1)$, X_{I}, and X_{II}. The equations are best solved numerically and give values as in Table 4.

Appendix D

Solutions for Region II *for* $\gamma = 7/5$ *under Conditions of Recondensation*

We again assume conditions of *recondensation* and write Ψ as follows

$$\Psi = \frac{F'(5A+U)}{A^2} - \frac{F(5A+U)}{5A^3} = \sum \frac{5nC_n(5A+U)^{n-1}}{A^2} - \sum \frac{C_n(5A+U)^n}{A^3} , \qquad \text{(D1)}$$

as is easily justified by substitution into (C1).

The constants C_n can be deduced by evaluating (C2) and (C3) in terms of (D1) at $\check{X}$ and X_{II}. The argument follows closely that for $\gamma = 5/3$. For example, as seen in Table 9, there are six conditions and we therefore need six constants. Furthermore, since (C2) and (D1) together give

$$25A^2F'' - 15AF' + 3F = 25A^5\Upsilon ,$$

we choose $n = 5$ and the constants become C_0, C_1, C_2, C_3, C_4, and C_5. It is easily shown that the following values are required:

$$C_5 = 0.0001 , \quad C_4 = 0 , \quad C_3 = -0.006 ,$$
$$C_2 = -0.008 , \quad C_1 = 0.096 , \quad C_0 = 0.2304 ,$$

and the expression for $F(5A+U)$ is therefore

$$F(5A+U) = 5\sum_0^5 C_n(5A+U)^n . \qquad \text{(D2)}$$

As with $\gamma = 5/3$ there is no additional information at $X = 0(\Upsilon = 1)$. In contrast to $\gamma = 5/3$, however, we find that the above set of constants *does not describe* the simple form of X_{I} seen in (13) (Table 9 and Appendix E). The C_n are easily shown to be correct by substituting $F(5A+U)$ into the six conditions.

The actual solutions are as follows. From $X = U\Upsilon - \partial\Psi/\partial U$, with Ψ as in (D1), one obtains

$$\begin{aligned}2000A^3X - 2000A^3U\Upsilon &= -20A(5A+U)^3 + 360A(5A+U) + 160A \\ &\quad + (5A+U)^4 - 36(5A+U)^2 - 32(5A+U) \\ &\quad + 192 . \end{aligned} \qquad \text{(D3)}$$

From $5A\Upsilon = \partial\Psi/\partial A$ one obtains

$$\begin{aligned}50{,}000A^5\Upsilon &= 500A^2(5A+U)^3 - 9000A^2(5A+U) - 4000A^2 \\ &\quad - 75A(5A+U)^4 + 2700A(5A+U)^2 \\ &\quad + 2400A(5A+U) - 14{,}400A + 3(5A+U)^5 \\ &\quad - 180(5A+U)^3 - 240(5A+U)^2 + 2880(5A+U) \\ &\quad + 6912 . \end{aligned} \qquad \text{(D4)}$$

Numerical solutions of (D3) and (D4) are given in Table 4.

To obtain information on the first LOC at X_{I}, we introduce $5A + U = 4$ into (D3) and (D4) and thus obtain

$$125A^3X - 125A^3U\Upsilon = 20A - 16 , \qquad \text{(D5)}$$
$$3125A^5\Upsilon = -500A^2 + 1200A + 384 . \qquad \text{(D6)}$$

Equations (D5) and (D6) can be rearranged to

$$X = U\Upsilon - (16 - 20A)/125A^3 , \qquad \text{(D7)}$$
$$A^5\Upsilon = 1024/3125 - (100A^2 - 240A + 128)/625 , \qquad \text{(D8)}$$

results which show the approximations of (13) to indeed be reasonable. The simplifications seen in (D5–D8) were not carried out with (A12) and (A13) of [2]. The latter equations are, however, otherwise correct.

Appendix E

Validity of the Simple Forms of (12–16) for Region I

We have noted that the somewhat complicated analytical solutions for region I under conditions of *reflection* as given in [2] can be approximated by the simple forms of (12–16). We here consider more closely the validity of the latter.

If the simple forms are valid for $\gamma = 5/3$ then the first LOC at X_{I} is described by (13):

$$A_{\mathrm{I}} = \frac{2}{3}\Upsilon^{-1/3} , \quad U_{\mathrm{I}} = 2 - 2\Upsilon^{-1/3} ,$$
$$3A_{\mathrm{I}} + U_{\mathrm{I}} = 2 .$$

The existence of the first LOC establishes two more conditions beyond the four used in Appendix C (see Table 9). In fact $F(3A+U)$ as in (C5) does satisfy the additional conditions and we conclude that the simple forms are valid.

Similarly, if the simple forms can be used for $\gamma = 7/5$ then again the first LOC is described by (13):

$$A_{\mathrm{I}} = \frac{4}{5}\Upsilon^{-1/5} , \quad U_{\mathrm{I}} = 4 - 4\Upsilon^{-1/5} ,$$
$$5A_{\mathrm{I}} + U_{\mathrm{I}} = 4 .$$

It is now found that there are three more conditions beyond the six used in Appendix D (see Table 9). Furthermore, $F(5A + U)$ as in (D2) satisfies none of the additional conditions and we conclude that the simple forms cannot be used now. Such a failure was suspected previously [16], but not proven.

Although the simple forms for region I are not generally valid, they are still useful for estimating A, U, and X_I (Tables 6 and 7). Estimating P is less successful since it involves a high power of A, while estimating the total quantity of particles in region I, Q_I, is unacceptable. Let us now consider Q_I.

Written in terms of the simple solution, Q_I is given by

$$Q_\mathrm{I} = A^{2/(\gamma-1)} X_\mathrm{I} = \left(\frac{3-\gamma}{2} \Upsilon^{-(\gamma-1)/2} \right)^{2/(\gamma-1)} X_\mathrm{I} .$$

X_I is described in general by (13a) and for large Υ by

$$X_\mathrm{I} \sim \frac{3-\gamma}{\gamma-1} \Upsilon .$$

The large-time, i.e. large-Υ, limit of Q_I follows as

$$\hat{Q}_\mathrm{I} \sim \frac{2}{\gamma-1} \left(\frac{3-\gamma}{2} \right)^{(\gamma+1)/(\gamma-1)} . \tag{E1}$$

It follows from (E1) that $\hat{Q}_\mathrm{I}$ is given by 0.593 for $\gamma = 5/3$, which is acceptable, but exceeds unity for all other γ. Since the largest possible value of $\hat{Q}_\mathrm{I}$ is 1.0, we conclude that the simple forms are unusable for treating Q_I starting at $\gamma = 7/5$.

The reason for the failure of the simple forms can be shown to lie in the *form* of the function F such as that seen in (D2) starting with $\gamma = 7/5$.

Appendix F

Corrections to [6]

The following two changes serve to make the notation of [6] consistent with the present work:
in (13b) replace u_I with $u_\mathrm{I} + a_\mathrm{I}$;
in (14b) replace u_II with $u_\mathrm{II} + a_\mathrm{II}$.

The following four changes arise because the quantity A_0^ref as in the present (11b) was taken as $(\gamma + 1)/4$, a distinction which does not matter for $\gamma = 5/3$:
in (12b, 12c, 13a, 13b) replace $(\gamma + 1)/4$ with $(3 - \gamma)/2$.

References

1. A. Miotello, R. Kelly: Submitted to Appl. Phys.
2. D. Sibold, H.M. Urbassek: Phys. Fluids A **4**, 165 (1992)
3. K.P. Stanyukovich: *Unsteady Motion of Continuous Media* (Pergamon, London 1960) pp. 121, 147, 151
4. R. Kelly, A. Miotello, B. Braren, A. Gupta, K.G. Casey: Nucl. Instrum. Methods B **65**, 187 (1992)
5. R. Kelly: J. Chem. Phys. **92**, 5047 (1990)
6. R. Kelly, B. Braren: Appl. Phys. B **53**, 160 (1991)
7. T. Ytrehus: In *Rarefied Gas Dynamics*, ed. by J.L. Potter, Vol. II (AIAA, New York 1977) p. 1197
8. C. Cercignani: In *Rarefied Gas Dynamics*, ed. by S.S. Fisher, Vol. I (AIAA, New York 1981) p. 305
9. R. Kelly, R.W. Dreyfus: Surf. Sci. **198**, 263 (1988)
10. R. Kelly, R.W. Dreyfus: Nucl. Instrum. Methods B **32**, 341 (1988)
11. I. NoorBatcha, R.R. Lucchese, Y. Zeiri: J. Chem. Phys. **86**, 5816 (1987)
12. D.W. Snoke, W.W. Rühle, Y-C. Lu, E. Bauser: Phys. Rev. B **45**, 10979 (1992)
13. H.M. Urbassek, J. Michl: Nucl. Instrum. Methods B **22**, 480 (1987)
14. R. Kelly: Nucl. Instrum. Methods B **46**, 441 (1990)
15. B. Braren, K.G. Casey, R. Kelly: Nucl. Instrum. Methods B **58**, 463 (1991)
16. R. Kelly: Phys. Rev. A **46**, 860 (1992)
17. L. Wiedeman, H. Helvajian: J. Appl. Phys. **70**, 4513 (1991)
18. D.L. Singleton, G. Paraskevopoulos, R.S. Irwin: J. Appl. Phys. **66**, 3324 (1989)
19. D.L. Singleton: National Research Council of Canada, Ottawa (personal communication, 1992)
20. A. Miotello, R. Kelly, B. Braren, C. Otis: Appl. Phys. Lett. **61**, 2784 (1992)
21. K.L. Saenger: J. Chem. Phys. **75**, 2467 (1981)
22. D. Sibold, H.M. Urbassek: Phys. Rev. A **43**, 6722 (1991)
23. R.E. Grundy: Phys. Fluids **12**, 2011 (1969)
24. J.C.S. Kools, T.S. Baller, S.T. de Zwart, J. Dieleman: J. Appl. Phys. **71**, 4547 (1992)
25. H.M. Urbassek, D. Sibold: Phys. Rev. Lett. **70**, 1886 (1993)
26. A. Vertes, P. Juhasz, M. de Wolf, R. Gijbels: Int. J. Mass Spectrom. Ion Processes **94**, 63 (1989)
27. A. Vertes, P. Juhasz, L. Balazs, R. Gijbels: In *Microbeam Analysis – 1989*, ed. by P.E. Russell (San Francisco Press, San Francisco 1989) p. 273
28. T. Ytrehus, J. Alvestad: In *Rarefied Gas Dynamics*, ed. by S.S. Fisher, Vol. I (AIAA, New York 1981) p. 330
29. R. Mager, G. Adomeit, G. Wortberg: In *Rarefied Gas Dynamics: Physical Phenomena*, ed. by E.P. Muntz, D.P. Weaver, D.H. Campbell (AIAA, Washington, DC 1988) p. 460
30. A. Dervieux, G. Vijayasundaram: In *Numerical Methods for the Euler Equations of Fluid Dynamics*, ed. by F. Angrand et al. (SIAM, Philadelphia 1985) pp. 121-144
31. R.D. Richtmyer, K.W. Morton: In *Difference Methods for Initial-Value Problems*, 2nd edn. (Interscience, New York 1967) pp. 330–345

Responsible for Advertisements: E. Lückermann, K. Schilling, Heidelberger Platz 3, D-14197 Berlin, Tel. (0 30) 82 07-0, Telex 01-85411, Fax (0) 30/8207300
Responsible for the Text: H. K. V. Lotsch, Tiergartenstraße 17, D-69121 Heidelberg, Tel. (0) 62 21/48 72 53, Telex 461723, Fax (0) 6221/43982
Printers: Brühlsche Universitätsdruckerei, Giessen

Springer-Verlag GmbH & Co. KG, D-14197 Berlin